2024 IEEE International Conference on Robotics and Automation (ICRA 2024)
May 13-17, 2024. Yokohama, Japan

Increasing the Absolute Position Accuracy of Industrial Robots by Means of a Deep Continual Evidential Regression Model*

Eckart Uhlmann, Mitchel Polte, Julian Blumberg, Sheng Yin, Gang Wang

Abstract— **The use of industrial robots represents a key technology for increasing productivity and efficiency in manufacturing. However, their low absolute position accuracy still denies the broad substitution of machine tools by industrial robots. In this paper, a data-driven method for accuracy enhancement of industrial robots under consideration of kinematic, elastic, and thermal effects is presented. A continual learning algorithm is proposed, which allows to train the model in a process-parallel manner without suffering from catastrophic forgetting. Furthermore, the model is able to determine confidence intervals of the prediction values and thus supports further processing in safety-relevant applications. The effectiveness of the model can be demonstrated using a large data stream with about 3,000 real data points. As a result, it can be shown that the absolute position accuracy of the industrial robot can be improved by 96 % with the proposed method.**

I. Introduction

Industrial robots are regarded as a key technology for the automation and flexibilization of production processes. They are consequently predestined to address crisis situations as well as challenges posed by the shortage of skilled workers. In this context, the Corona pandemic can be seen as an additional driver for the record number of 510 thousand new industrial robots installed in the field in 2022, which represents an increase of 31 % compared to 2020 [1]. With 64 thousand newly installed industrial robots in 2022, the metal and machinery industry is the third largest customer behind the electrical/electronics and automotive industries [1]. The substitution of machine tools by industrial robots holds great potential for further increase in this sector [2].

Currently, it is primarily the low absolute position accuracy T of industrial robots that prevents their widespread use for manufacturing processes [3]. Many research activities focus on methods to increase the absolute position accuracy T in terms of robot design [4], robot control [5,6] or robot calibration [7,8]. The latter approach aims to identify a model that describes the real relationship between joint angles **q** and pose **P** of the industrial robot. This model includes kinematic parameters, e. g. according to the Denavit-Hartenberg convention, and is successively extended for higher accuracies by parameters describing gear, bearing and structural stiffness, gear backlash and/or thermal expansions [9-11].

*Research supported by European Union.

E. Uhlmann, M. Polte, J. Blumberg, and S. Yin are with the Institute for Machine Tools and Factory Management IWF, Technische Universität Berlin, Pascalstr. 8-9, 10587 Berlin, Germany (phone: +49 30 314 244 52; e-mail: blumberg@iwf.tu-berlin.de).

G. Wang is with the State Key Laboratory of Mechanical Transmission, College of Mechanical and Vehicle Engineering, Chongqing University, Chongqing 400044, China.

However, these models are always limited by simplifying assumptions as well as complex parameter identification methods [12]. Furthermore, the complexity of such models can hinder their feasibility in real-time applications. Alternative approaches focus on the use of black box models in terms of a machine learning regression problem [13-15]. The accuracy of such data-driven models strongly depends on the availability of large data sets D. In particular, with increasing dimensionality in the input space, larger amounts of data have to be provided for training. The simultaneous consideration of the kinematic, elastic, and thermal behavior of industrial robots has not been investigated yet. Model training is generally based on a batch method, i. e. data generation is always upstream of model training and model training is based on all training data simultaneously. Continual learning methods, where a data stream is processed successively, represent a paradigm shift in the field of training data-driven models. The goal is to retain stability in the sense of already learned knowledge while the model has enough plasticity to learn new contexts. To the best of our knowledge, this is the first paper that presents a method for continual learning in the context of robot calibration. Data-driven models in general suffer from over- or under-confidence. Without knowledge about the uncertainty of the model, i. e. the epistemic uncertainty, the use of such models in safety-relevant areas is critical. In addition, there is uncertainty in the measured data, i. e. the aleatoric uncertainty, which further reduces the prediction accuracy of such models. An evidential regression model is used in this paper that accounts for epistemic and aleatoric uncertainty without relying on a Bayesian approach or repeated training. In summary, the specific contributions of the paper are as follows:

- fully comprehensive robot calibration in terms of kinematic, elastic, and thermal behavior,
- prediction of confidence interval based on a Normal Inverse Gamma distribution loss function for Artificial Neural Networks (ANN), and
- replay-based continual learning for ANN models with a maximum error selection strategy in order to minimize catastrophic forgetting.

II. Related Work

The objective in a data-driven robot calibration is to find a function f based on a data set $D = \{\mathbf{x}_i, \mathbf{y}_i \mid i = 1,\ldots,N\}$ such that an error function $\boldsymbol{\epsilon}$ gets minimized:

$$\mathbf{y}_i = f(\mathbf{x}_i) + \boldsymbol{\epsilon}_i \quad , \quad \mathbf{x}_i \in \mathbb{R}^m, \mathbf{y}_i \in \mathbb{R}^n \tag{1}$$

where $\mathbf{x}_i$ and $\mathbf{y}_i$ are the input or feature and output or label vectors of dimensions m and n, respectively. To increase the

accuracy of industrial robots, mainly ANN and Gaussian process regressions (GPR) were investigated due to their ability to approximate arbitrary nonlinear relationships as well as their flexibility and learning ability [16,17]. Further, the suitability of Support Vector Regression (SVR), Extreme Learning Machine (ELM), and Fuzzy Interference Systems (FIS) for increasing the accuracy of industrial robots has been demonstrated [18-20]. However, besides the choice of the machine learning model and the corresponding hyperparameters, especially the size N of the data set *D* as well as the definition of the features $\mathbf{x}_i$ and labels $\mathbf{y}_i$ are the limiting factors for the accuracy increase. Most works use the joint angles $\mathbf{q}$ as features $\mathbf{x}_i$ and the position error $\mathbf{e}_{Pos}$ or full pose error $\mathbf{e}_P$ to a calibrated robot model as labels $\mathbf{y}_i$ [13,16]. In this way, the kinematic behavior can be described as a function of the joint angles $\mathbf{q}$. Alternative labels include the absolute real pose $\mathbf{P}$ and the relative pose error $\mathbf{e}_P$ to the uncalibrated robot model. UHLMANN ET AL. [21] have shown that the relative pose error $\mathbf{e}_P$ to the uncalibrated robot model provides the best results, which makes a conventional robot calibration unnecessary. By considering an additional feature $\mathbf{x}_i$ for the payload P_L mounted at the end effector, the stiffness behavior in gravity direction can be captured [22]. With the six components of the complete force-torque vector $\mathbf{W}$ acting at the end effector as additional features $\mathbf{x}_i$, the pose-dependent stiffness can be modeled in all Cartesian spatial directions [17,20]. So far, the complete force-torque vector $\mathbf{W}$ is only considered in conjunction with the deformation error $\boldsymbol{\delta}_F$ as the labels $\mathbf{y}_i$. Thus, the model is not capable to capture kinematic error sources. Research on capturing the thermal behavior of industrial robots through data-driven models is currently not known.

All of the above methods for data-driven robot calibration are based on a batch method for training, i. e. all training data is presented to the model simultaneously. Continual learning is a promising approach to overcome time-consuming learning phases as well as to consider changes in the input and output domain. Currently, continual learning algorithms can be classified into three main categories: (1) Regularization-based approach [23], (2) Dynamic architecture-based approach [24], and (3) Replay-based approach [25]. Mainly such methods are used to solve image classification tasks. Due to simplicity and robustness, the Incremental Classifier and Representation Learning (iCaRL) algorithm by REBUFFI ET AL. [25] is adopted here for continual learning in a regression problem. It is a replay-based algorithm with a fixed memory size N_m for storing exemplars from previous data. The goal is to find representative data for the memory that will prevent catastrophic forgetting while allowing for rapid adaptability. In this paper a maximum error selection strategy is proposed.

III. ARTIFICIAL NEURAL NETWORK MODEL

A. Loss function

The basis for the investigations in this paper is the evidential regression model proposed by AMINI ET AL. [26]. The model aims to approximate the Normal Inverse Gamma (NIG) distribution according to:

$$\begin{aligned} \mathrm{NIG}(\gamma, \nu, \alpha, \beta) = \; & \frac{\beta^{\alpha}\sqrt{\nu}}{\Gamma(\alpha)\sqrt{2\pi\sigma^2}}\left(\frac{1}{\sigma^2}\right)^{\alpha+1} \\ & \cdot \exp\left\{-\frac{2\beta + \nu(\gamma - \mu)^2}{2\sigma^2}\right\} \end{aligned} \tag{2}$$

where $\Gamma(\cdot)$ is the gamma function, μ and σ^2 the unknown mean and variance, and $\mathbf{m} = [\gamma, \nu, \alpha, \beta]$ are the parameters of the NIG distribution with $\gamma \in \mathbb{R}$, $\nu > 0$, $\alpha > 1$ and $\beta > 0$. The parameters $\mathbf{m}$ can be used to compute the prediction $\mathbb{E}[\mu]$ as well as the aleatoric $\mathbb{E}[\sigma^2]$, and epistemic uncertainty $\mathrm{Var}[\mu]$ by:

$$\mathrm{E}[\mu] = \gamma, \quad \mathrm{E}[\sigma^2] = \frac{\beta}{\alpha - 1}, \quad \mathrm{Var}[\mu] = \frac{\beta}{\nu(\alpha - 1)} \tag{3}$$

In this paper a fully connected Multi-Layer Perceptron (MLP) ANN is used to predict the four parameters $\mathbf{m}$ for each component of the pose error $\mathbf{e}_P$ to the uncalibrated industrial robot. Preliminary investigations have shown that separate models for each component of the pose error $\mathbf{e}_P$ provide superior results. In total six models with four output parameters $\mathbf{m}$ each are trained. According to AMINI ET AL. [26] the parameters $\mathbf{m}$ of the NIG distribution can be trained by means of a multi-task learning problem. In the first step the model prediction accuracy is maximized, which is formulated by marginalizing over the likelihood parameters. The loss L^{NLL} is defined by the negative logarithm of the model evidence:

$$\begin{aligned} L^{NLL}(\mathbf{w}) = \; & 0.5 \cdot \log\left(\frac{\pi}{\nu}\right) - \alpha \log(\Omega) \\ & + (\alpha + 0.5)\log((y - \gamma)^2\nu + \Omega) \\ & + \log\left(\frac{\Gamma(\alpha)}{\Gamma(\alpha + 0.5)}\right) \end{aligned} \tag{4}$$

where $\mathbf{w}$ are the weights, y are the true labels, and $\Omega = 2\beta(1+\nu)$. In the second step the evidence on prediction errors is minimized, which is done by introducing a penalty term in form of a regularizer L^R:

$$L^R(\mathbf{w}) = |y - \gamma| \cdot (2\nu + \alpha) \tag{5}$$

The total loss $L(\mathbf{w})$ is composed by (4) and (5) as in:

$$L(\mathbf{w}) = L^{NLL}(\mathbf{w}) + \lambda \cdot L^R(\mathbf{w}) \tag{6}$$

where λ is the regularization coefficient, which can be seen as a trade-off between over- and under-confidence.

B. Hyperparameter optimization

Hyperparameters $\boldsymbol{\Lambda}$, such as number of hidden layers N_h, neurons per hidden layer N_n, batch-size n_B, dropout-rate d, and learning rate η, directly affect model training and performance. The choice of hyperparameters $\boldsymbol{\Lambda}$ is therefore crucial to achieve high absolute position accuracy T of industrial robots. In this paper, the hyperparameters $\boldsymbol{\Lambda}$ are optimized using Optuna in Python 3.9. For parameter identification the sequential model-based optimization algorithm called Tree-structured Parzen Estimator [27] is used. The algorithm utilizes a regression model rooted in historical evaluations of hyperparameters $\boldsymbol{\Lambda}$ with the goal to find hyperparameters $\boldsymbol{\Lambda}$ that maximize the history-dependent

TABLE I. HYPERPARAMETER SEARCH SPACE

hyperparameter	sampling distribution	bounds / parameter set
number of hidden layers N_h	uniformly	[1, 15]
neurons per hidden layer N_n	uniformly	[50, 500]
activation function	-	["ELU", "ReLU", "GELU"
batch size n_B	uniformly	[4, 64]
learning rate η	log-uniformly	$[10^{-7}, 10^{-2}]$
weight decay w_d	log-uniformly	$[10^{-7}, 10^{-2}]$
dropout rate d	uniformly	[0.0, 0.5]

criterion called Expected Improvement [27]. The search space is summarized in Tab. 1.

C. Continual learning

The continual learning method proposed here is a replay-based method, i. e. each time new data arrives the training is repeated for a fixed memory size N_m. Let's assume the features and labels stored in the current memory are $\mathbf{X}_i \in \mathbb{R}^{m \times N_m}$ and $\mathbf{Y}_i \in \mathbb{R}^{n \times N_m}$, with m and n as the dimensions of the feature and label space. New data is denoted as $\mathbf{x}^* \in \mathbb{R}^{m \times n_B}$ and $\mathbf{y}^* \in \mathbb{R}^{n \times n_B}$, with n_B as the batch-size processed in one iteration of continual learning. The goal is to find a subset of features $\mathbf{X}_{i+1} \subset \{\mathbf{X}_i, \mathbf{x}^*\}$ with corresponding labels $\mathbf{Y}_{i+1}$, where $\mathbf{X}_{i+1} \in \mathbb{R}^{m \times N_m}$ and $\mathbf{Y}_{i+1} \in \mathbb{R}^{n \times N_m}$. In the aim of a high achievable absolute position accuracy T of the industrial robot, a subset should be chosen so that maximum performance of the model is guaranteed. Based on that, predictions are made in each iteration for data in the current memory $\mathbf{X}_i$ as well as new data $\mathbf{x}^*$ with the current model M_i. Errors between the true labels $\mathbf{Y}_i$ and $\mathbf{y}^*$ as well as the predicted values ${}^{P}\mathbf{Y}_i$ and ${}^{P}\mathbf{y}^*$ are calculated as the Euclidean distance and stored in a complete error vector $\mathbf{E}_i$, as in:

$$\mathbf{E}_i = \{\mathbf{E}_X, \mathbf{E}_x\},\ \mathbf{E}_X = \sqrt{\left(\mathbf{Y}_i - {}^{P}\mathbf{Y}_i\right)^2},\ \mathbf{E}_x = \sqrt{\left(\mathbf{y}^* - {}^{P}\mathbf{y}^*\right)^2} \quad (7)$$

The new memory with features $\mathbf{X}_{i+1}$ and labels $\mathbf{Y}_{i+1}$ is chosen by sorting the complete error vector $\mathbf{E}_i$ in descending order and selecting the first N_m data points, i. e. data points with the largest error. The updated model M_{i+1} is obtained by training on the updated data set $D = \{\mathbf{X}_{i+1}, \mathbf{Y}_{i+1}\}$. This maximum error selection strategy prevents catastrophic forgetting, since the error of previous tasks immediately grows when changing domains in the feature space. For the same reason, this approach also has a high plasticity for learning new tasks.

IV. EXPERIMENTAL DATA ACQUISITION

Throughout the remaining paper the industrial robot M-900iB/700 from the company FANUC K.K., Oshino, Japan with a nominal payload of P = 700 kg serves as a demonstrator. The industrial robot is equipped with a parallelogram-mechanism, spring-based gravity compensators as well as secondary encoders at all six axes, see Fig. 1. Extensive measurement data of the pose, i. e. position and orientation, is recorded from the M-900iB/700 with the laser tracker AT960 in combination with a T-Mac sensor from the company HEXAGON AB, Stockholm, Sweden. The system has an absolute distance accuracy of 15 µm for distances of up to 10 m [28]. To record the physical effects influencing the

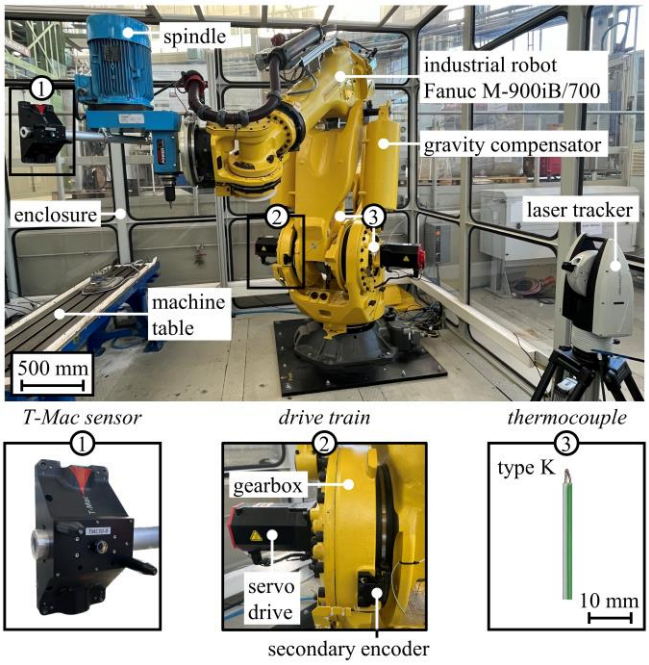

Figure 1. Measurement set-up with Fanuc M-900iB/700

absolute position accuracy T as precisely as possible, the following points should be considered for data acquisition:

- utilization of the entire working space of the robot,
- use of different robot configurations (elbow up/down, etc.), and
- passing through backlash as frequently as possible in all six axes.

The three above mentioned aspects are directly incorporated by randomly choosing joint angles $\mathbf{q}$ under consideration of axis limitations. However, random joint angles $\mathbf{q}$ will most likely result in movements that do not ensure laser tracker sensor visibility as well as cause collisions with the environment. Therefore, a method based on Fig. 2 is developed, which allows to check the laser tracker sensor visibility in advance. The measured pose is represented as a homogeneous transformation matrix ${}^{S}_{W}\mathbf{T}$ pointing from the world frame {W} to the sensor frame {S}, as in:

$${}^{S}_{W}\mathbf{T} = \begin{pmatrix} {}^{S}_{W}\mathbf{R} & {}^{S}_{W}\mathbf{p} \\ \mathbf{0} & 1 \end{pmatrix} = \begin{pmatrix} {}^{S}_{W}\mathbf{x} & {}^{S}_{W}\mathbf{y} & {}^{S}_{W}\mathbf{z} & {}^{S}_{W}\mathbf{p} \\ 0 & 0 & 0 & 1 \end{pmatrix} \quad (8)$$

where ${}^{S}_{W}\mathbf{R} = ({}^{S}_{W}\mathbf{x}, {}^{S}_{W}\mathbf{y}, {}^{S}_{W}\mathbf{z}) \in SO(3)$ is the orthogonal rotation matrix with its elementary axes and ${}^{S}_{W}\mathbf{p} \in \mathbb{R}^3$ the position vector. The homogeneous transformation matrix ${}^{S}_{W}\mathbf{T}$ can be predicted a priori by:

$${}^{S}_{W}\mathbf{T}_{calc} = {}^{W}_{0}\mathbf{T}^{-1} \cdot {}^{6}_{0}\mathbf{T}(\mathbf{q}) \cdot {}^{S}_{6}\mathbf{T} \quad (9)$$

where ${}^{6}_{0}\mathbf{T} = f(\mathbf{q})$ represents the forward kinematics of the industrial robot in dependence of the joint angles $\mathbf{q}$. To identify the homogeneous transformation matrices ${}^{W}_{0}\mathbf{T}$ and ${}^{S}_{6}\mathbf{T}$ the well-studied hand-eye calibration of the form $\mathbf{AX} = \mathbf{ZB}$ must be solved [29]. The T-Mac sensor has a field of view of $\alpha_{max} = 45°$ about the perpendicular axis of the reflector, which is represented by the local Z-axis z_S. The angle between the T-Mac sensor and the laser tracker follows a priori by:

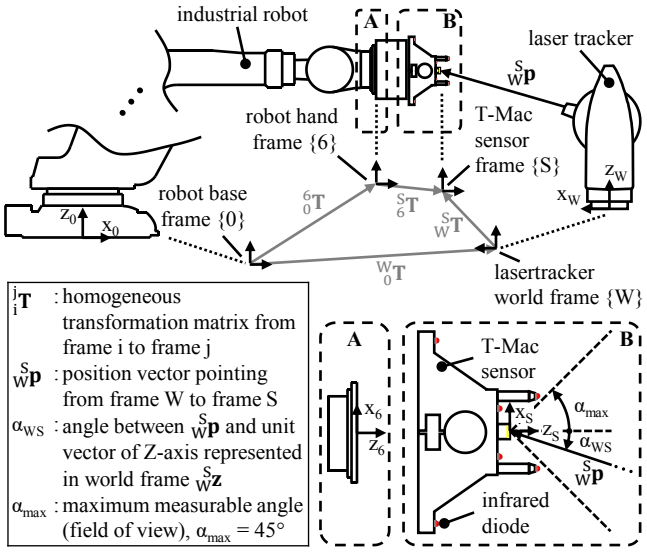

Figure 2. Method to check for laser tracker sensor visibility

$$\alpha_{WS} = f(\mathbf{q}) = \cos^{-1}\left(\frac{{}^{S}_{W}\mathbf{p}_{calc} \cdot {}^{S}_{W}\mathbf{z}_{calc}}{||{}^{S}_{W}\mathbf{p}_{calc}|| \cdot ||{}^{S}_{W}\mathbf{z}_{calc}||}\right) \quad (10)$$

The feasibility of randomly generated joint angles $\mathbf{q}$ in terms of the laser tracker measurements is given, if $\alpha_{WS} \leq \alpha_{max}$ holds true. In addition, the Euclidean norm of the position vector must be $||\mathbf{p}_{ws}|| \geq 1.5$ m in order to guarantee a minimum distance between the laser tracker and the T-Mac sensor.

Further, collisions with the environment as well as self-collisions for randomly generated joint movements are monitored using the Robotics System Toolbox in Matlab 2023a from THE MATHWORKS, INC., Natick, USA. The Unified Robot Description Format (URDF) file by ROS-Industrial support for Fanuc manipulators is used to build the convex hull of the robot [30]. The enclosure, the machine table, and the spindle are modeled as convex cuboids, cylinders, and spheres, see Fig. 3. Collisions are checked for the entire trajectory in terms of synchronous joint movements between the discrete measurement points.

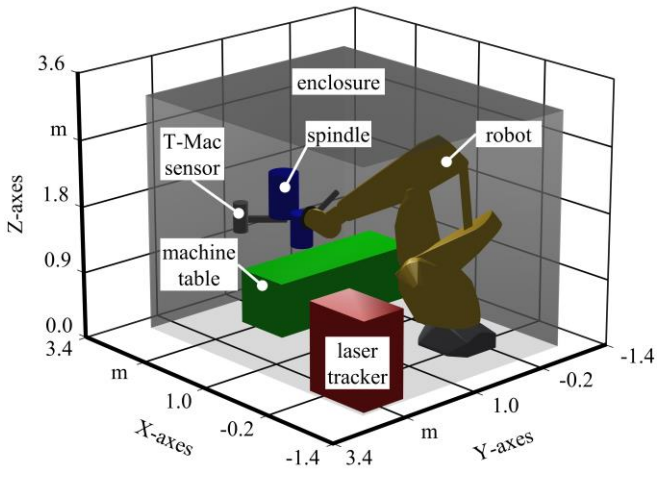

Figure 3. Collision simulation

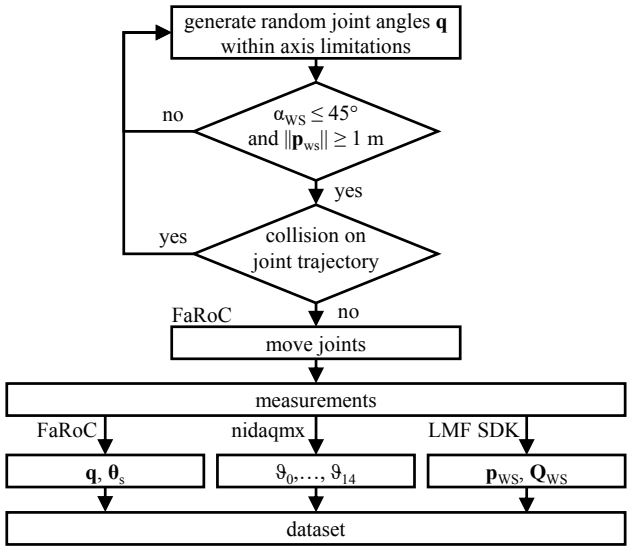

Figure 4. Automated measurement procedure

The measurements are fully automated using Python 3.9. A reading and writing communication based on EhterNet/IP-protocol to an R-30iB robot controller by the company FANUC K.K., Oshino, Japan, is implemented. It is available under the acronym FaRoC (Fanuc Robot Control) [31]. FaRoC is used to move the robot in joint space. Further, the measured joint angles of the secondary encoders $\boldsymbol{\theta}_s$ are recorded. According to UHLMANN ET AL. [32] the difference between the nominal joint angles $\mathbf{q}$ and the joint angles of the secondary encoders $\boldsymbol{\theta}_s$ can be used as a measure for the external force-torque vector $\mathbf{W}$.

Temperatures $\boldsymbol{\vartheta}$ of the robot structure are measured with the temperature measurement module NI-9213 mounted in the compact DAQ chassis cDAQ-9174 by NATIONAL INSTRUMENTS COOPERATION, Austin, USA, and 14 thermocouples of type K by THERMA THERMOFÜHLER GMBH, Lindlar, Germany. The thermocouples are mounted either close to the servo drives or close to the joints. In addition, one thermocouple is used to capture ambient temperature ϑ_0. Data acquisition is automated by using the *nidaqmx* package as an Application Programming Interface (API) for interacting with the NI-DAQmx driver. The laser tracker measurements are automated with the Leica Metrology Foundation Software Development Kit (LMF SDK). The LMF SDK can be included into a Python environment using the *pythonnet* package. The full measurement procedure is summarized in Fig. 4.

In total N = 3,004 datapoints are recorded within the intervals according to Tab. 2. The absolute position accuracy T is defined as the Euclidean distance between the nominal kinematic model and the measured data. It is shown for the N = 3,004 datapoints in Fig. 5. The average absolute position accuracy is $\overline{T} = 2.77$ mm with a maximum error of $T_{max} = 10.25$ mm and a standard deviation of $T_{std} = 0.84$ mm. For the sake of simplicity, only position data are stated

TABLE II. FEATURE DISTRIBUTION

	θ_1 in °	θ_2 in °	θ_3 in °	θ_4 in °	θ_5 in °	θ_6 in °	ϑ in °C
min	-26.7	-45.4	-79.8	-157.1	-102.2	-174.0	23.5
max	98.8	72.4	25.0	166.5	110.4	180.0	75.4

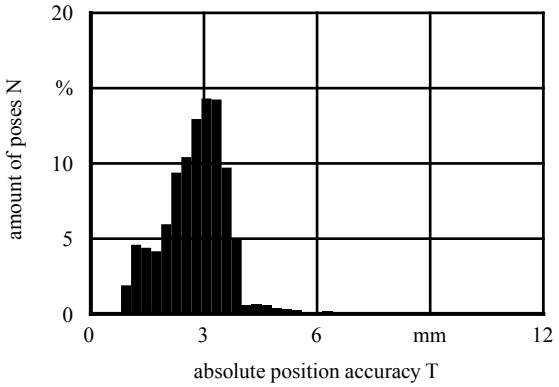

Figure 5. Error histogram of uncalibrated robot for N = 3,004 data points

throughout the paper, although investigations were also carried out with orientation data. The modeling procedure as well as the results and conclusions are equivalent. It is worth mentioning that the measured data include poses near the axis limitations and is partially recorded under severe external force application of up to $\|\mathbf{F}\| \leq 3{,}000$ N, applied by an air spring, as well as thermal loads with temperature differences of $\Delta\vartheta < 55$ K induced by the servo motors after extensive warm-up movements. Further, the data was acquired on different days with different setups of the laser tracking system in order to guarantee robustness and transferability.

V. RESULTS AND DISCUSSION

Given is a data set $D = \{\mathbf{x}_i, \mathbf{y}_i \mid i = 1,\ldots,N\}$ with N = 3,004 data points. The input vector consists of six joint angles $\mathbf{q}$, six elastic joint deformations $\boldsymbol{\Delta\theta}$, and 15 temperatures $\boldsymbol{\vartheta}$. The output vector contains the six components of the pose error $\mathbf{e}_P$ to the uncalibrated robot model, each modelled with the four parameters $\mathbf{m}$ of the NIG distribution. The full ANN model with the aforementioned input and output vectors $\mathbf{x}_i$ and $\mathbf{y}_i$ is referred to as M_{full}. The input vector is scaled by a min-max normalization. The full data set D is divided randomly into a training and test data set, referred to as D_{train} and D_{test}, with a 90 % to 10 % ratio. All following results are based on the test data set D_{test} unknown to the models.

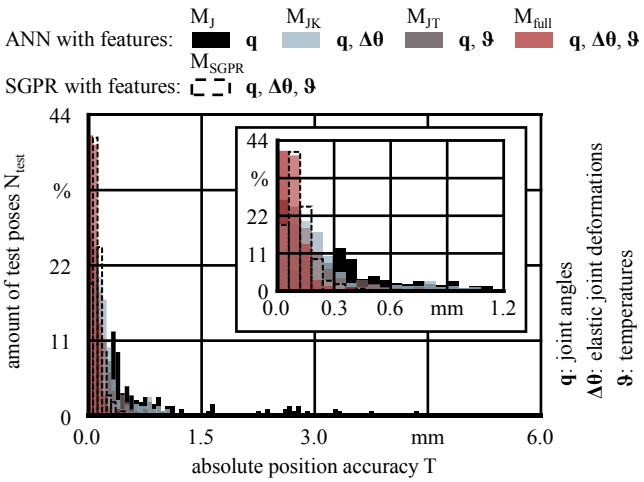

Figure 6. Result of models M_{full} and M_J on the test data set D_{test}

Fig. 6 shows the result of the full model M_{full} in comparison to models under consideration of different subsets of the input vector $\mathbf{x}_i$. A hyperparameter optimization is performed for each model separately. In addition, a Sparse Gaussian Process Regression (SGPR) model is trained with the complete input vector $\mathbf{x}_i$ in order to provide a benchmark. The average absolute position accuracy of the models are $\overline{T}_{M,full} = 0.08$ mm, $\overline{T}_{M,JK} = 0.27$ mm, $\overline{T}_{M,JT} = 0.16$ mm, $\overline{T}_{M,J} = 0.84$ mm, and $\overline{T}_{M,SGPR} = 0.12$ mm. The results show that both, elastic joint deformations $\boldsymbol{\Delta\theta}$ and temperatures $\boldsymbol{\vartheta}$ as additional inputs, contribute significantly to the model performance. Further, the proposed ANN model proves to be superior to the SGPR model as a benchmark.

Further investigations of the model include the dependency upon the amount of training data N_{train} drawn from the train data set D_{train}. As data acquisition remains a time-consuming task, models with lower need for training data are advantageous. Separate models were each trained with a subset of the train data set D_{train}. The results are shown in Fig. 7. The subset is chosen randomly in each case. Robustness is ensured by repeating the random selection ten times, which corresponds to the error bars in Fig. 7. It can be seen that the absolute position accuracy T is continuously improved with increasing amount of training data N_{train}. With $N_{train} = 500$ training data the average absolute position accuracy corresponds to $\overline{T} = 0.24$ mm, which is an improvement of 74.5 % compared to the model trained with $N_{train} = 100$ data. With $N_{train} = 2{,}704$ training data the average absolute position accuracy corresponds to $\overline{T} = 0.08$ mm, which is an improvement of 17.1 % compared to the model trained with $N_{train} = 2{,}000$ data. It can be seen from these investigations that the percentage increase in absolute position accuracy T decreases with an increasing amount of training data N_{train}. Since the repeatability of the industrial

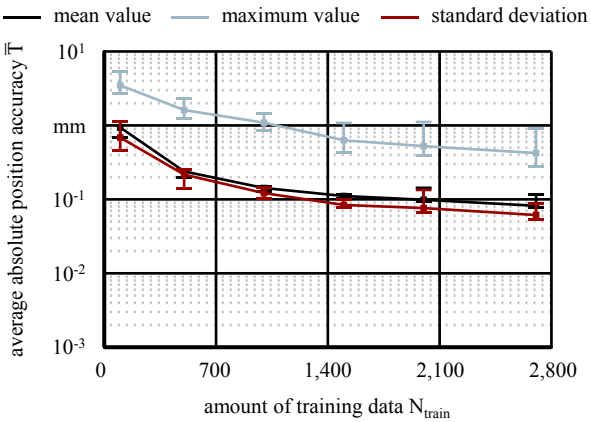

Figure 7. Dependency of model performance upon the amount of training data N_{train}

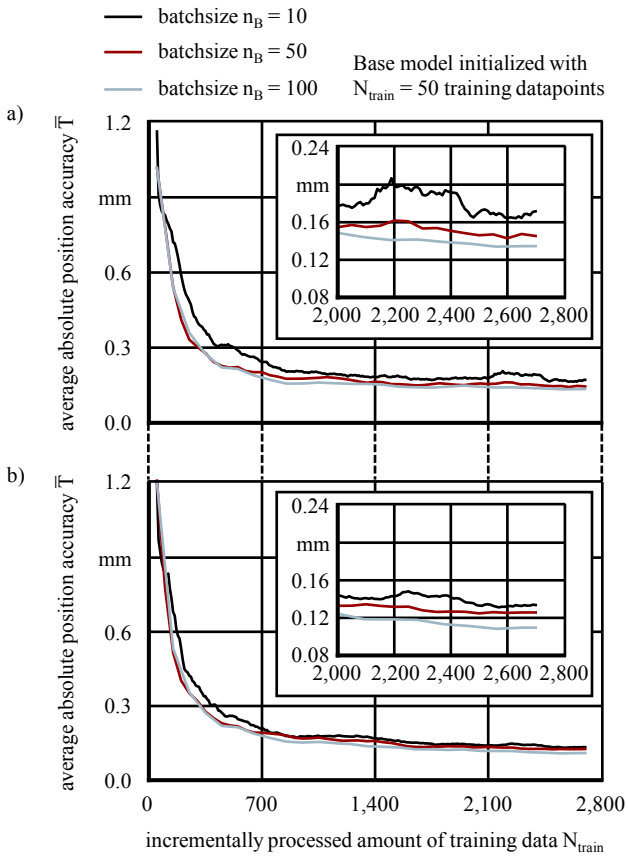

Figure 8. Results of continual learning on test data set D_{test}; a) memory size N_m = 200; b) memory size N_m = 500

robot is in the range of RP = 0.1 mm, it can be assumed that convergence has been achieved despite the increase in absolute position accuracy T between N_{train} = 2,000 and N_{train} = 2,704 training data.

To investigate continual learning based on the replay-based method, a model was initialized with a subset of N_{train} = 50 training data drawn from the training data set D_{train}. The model initialized in this way can be seen as poorly trained, revealing the effect of continual learning. The remaining data is successively provided to the model in the form of a continuous data stream. Batch sizes of n_B = 10, n_B = 50, and n_B = 100 were investigated, which corresponds to the amount of training data provided to the model in one iteration. Furthermore, the two memory sizes N_m = 200 and N_m = 500 were examined. The results achieved on the independent test data set D_{test} are shown in Fig. 8. It can be seen that the absolute position accuracy T of the industrial robot is continuously improved as the data stream increases. Larger batch sizes n_B achieve better results regardless of the memory size N_m. With larger batch sizes n_B, the information content as well as the variance in the data is more extensive, which gives the model more opportunities to select a memory with significant data points. This can improve the models learning and generalization ability. Furthermore, larger memory sizes N_m lead to better absolute position accuracy T. A larger memory size N_m means that the model can store more representative samples from previous tasks. This reduces catastrophic forgetting by retaining knowledge from previous data and ensuring that the model does not drift too far away from what it has previously learned. The memory size N_m as well as the batch size n_B should be chosen as a trade-off between model accuracy and available budget, e. g. in terms of computational power.

The model continually trained with a memory size of N_m = 500 and a batch size of n_B = 100 reaches an average absolute position accuracy of $\overline{T}$ = 0.11 mm on the independent test data set D_{test} after incrementally processing an amount of N_{train} = 2,704 training data. In comparison, the batch model, trained on same amount of training data simultaneously, achieves an average absolute position accuracy of $\overline{T}_{M,full}$ = 0.08 mm. Related to the uncalibrated industrial robot with an average position accuracy of $\overline{T}$ = 2.77 mm, this corresponds to accuracy losses of the continually trained model compared to the full batch model of about 1 %. The model with a memory size of N_m = 200 and a batch size of n_B = 10 has an accuracy loss of 3 % compared to the full batch model. A batch-model trained with an amount of training data of N_{train} = 500 randomly drawn from the train set D_{train}, as given in Fig. 7, achieves an average position accuracy of $\overline{T}$ = 0.24 mm (median value) and $\overline{T}$ = 0.20 mm (minimum value) over ten independent batch training repetitions. These results show that the training data in the memory of the continually trained model is more valuable for increasing the absolute position accuracy T of the industrial robot, which proves the effectiveness of the method.

VI. Conclusion

In this paper, a data-driven robot calibration is presented that considers the kinematic, elastic, and thermal behavior of industrial robots. The loss function of the model is based on a normal inverse gamma distribution, which enables the prediction of aleatoric as well as epistemic uncertainty in addition to point estimates. With a continual learning method data can be processed successively. The method is replay-based, i. e. model training is performed incrementally on a fixed memory. A maximum error selection strategy is proposed, in order to select data for the memory that achieve high absolute position accuracy T. Based on extensive experimental data from the Fanuc M-900iB/700, the model could increase the average absolute position accuracy to a range of 0.11 mm $\leq \overline{T} \leq$ 0.17 mm depending on the memory and batch size. This corresponds to an accuracy increase of between 94 % and 96 % to the uncalibrated robot with an accuracy loss below 3 % compared to the conventional batch training.

Acknowledgment

The depicted results were achieved to a great extent in the project “Monolithisches Laser-Sensor-Kalibriersystem für Industrieroboter” (Ref.-no. 10180397), which is co-financed by the European Union and supervised by the Investitionsbank Berlin.

REFERENCES

[1] C. Müller, "World Robotics 2022 – Industrial Robots," IFR Statistical Department, VDMA Services GmbH, Frankfurt am Main, Germany, 2022.

[2] E. Mühlbeier, P. Gönnheimer, L. Hausmann, J. Fleischer, "Value Stream Kinematics," in Proceedings of the 10th Congress of the German Academic Association for Production Technology (WGP), Dresden, 23-24 September, 2020.

[3] A. Verl, A. Valente, S. Melkote, C. Brecher, E. Ozturk, L.F. Tunc, "Robots in machinig," CIRP Annals, vol. 68, no. 2, pp. 799-822, 2019.

[4] Fraunhofer Society, "Flexmatik 4.1", URL: https://www.flexmatik.de/ (Access: 2023-08-03).

[5] S. Xiaoying, Z. Xiaojun, W. Pengyuan, H. Chen, "A review of robot control with visual servoing," in Proceedings of IEEE 8th Annual Conference on CYBER Technology in Automation, Control and Intelligent Systems, 2018, pp. 116-121.

[6] P. Gierlak, "Force control in robotics: A review of applications," Journal of Robotics and Mechanical Engineering, vol. 1, no. 1, pp. 1-5, 2021.

[7] A.Y. Elatta, L.P. Gen, F.L. Zhi, Y. Daoyuan, L. Fei, "An overview of robot calibration," Information Technology Journal, vol. 3, no. 1, pp. 74-78, 2004.

[8] G. Wang, W.L. Li, C. Jiang, D.H. Zhu, H. Xie, X.J. Liu, H. Ding, "Simultaneous calibration of multicoordinates for dual-robot systems by solving the AXB = YCZ problem," IEEE Transactions on Robotics, vol. 73, no. 4, pp. 1172-1185, 2021.

[9] K. Wu, J. Li, H. Zhao, Y. Zhong, "Review of industrial robot stiffness identification and modelling," Applied Sciences, 12, 8719, pp. 1-24, 2022.

[10] M. Cordes, W. Hintze, "Offline simulation of path deviation due to joint compliance and hysteresis for robot machining," International Journal for Advanced Manufacturing Technology, vol. 90, pp. 1075-1083, 2017.

[11] S. Reinkober, "Fräsbearbeitung von Nickelbasislegierungen mit Industrierobotern," Ph.D. dissertation, Faculty of Mechanical Engineering and Transport Systems, Technische Universität Berlin, Berlin, Germany, 2017.

[12] Z. Jiang, M. Huang, "Stable calibrations of six-DOF serial robots by using identification models with equalized singular values," Robotica, vol. 39, no. 12, pp. 1-22, 2021.

[13] H.N. Nguyen, J. Zhough, H.J. Kang, "A calibration method for enhancing robot accuracy through integration of an extended Kalman filter algorithm and an artificial neural network," Neurocomputing, vol. 151, no. 3, pp. 996-1005, 2015.

[14] A. Angelidis, G.C. Vosniakos, "Prediction and compensation of relative position error along industrial robot end-effector paths," Int. J. Precis. Eng. Manuf., vol. 15, no. 1, pp. 63-73, 2014.

[15] P.N. Le, H.J. Kang, "A robotic calibration method using a model-based identification technique and an invasive weed optimization neural network compensator," Applied Sciences, vol. 10, no. 20, pp. 1-14, 2020.

[16] H.N. Nguyen, P.N. Le, H.J. Kang, "A new calibration method for enhancing robot position accuracy by combining a robot model-based identification approach and an artificial neural network-based error compensation technique," Advances in Mechanical Engineering, vol. 11, no. 1, pp. 1-11, 2019.

[17] J. Blumberg, Z. Li, L.I. Besong, M. Polte, J. Buhl, E. Uhlmann, M. Bambach, "Deformation error compensation of industrial robots in single point incremental forming by means of data-driven stiffness model," in 26th International Conference on Automation and Computing, 2021, pp. 1-6.

[18] L. McGarry, J. Butterfield, A. Murphy, C. Higgins, "Machine learning methods to improve the accuracy of industrial robots," SAE Technical Paper, 2023-01-1000, 2023.

[19] P. Yuan, D. Chen, T. Wang, S. Cao, Y. Cai, L. Xue, "A compensation method based on extreme learning machine to enhance absolute position accuracy for aviation drilling robot," Advances in Mechanical Engineering, vol. 10, no. 3, pp. 1-11, 2018.

[20] S. Marie, E. Courteille, P. Maurine, "Elasto-geometrical modeling and calibration of robot manipulators: Application to machining and forming applications," Mechanism and Machine Theory, Elsevier, vol. 69, pp. 13-43, 2013.

[21] E. Uhlmann, M. Polte, J. Blumberg, Z. Li, A. Kraft, "Hyperparameter optimization of artificial neural networks to improve the positional accuracy of industrial robots," Journal of Machine Engineering, vol. 21, no. 2, pp. 47-59, 2021.

[22] X. Chen, Q. Zhang, Y. Sun, "Evolutionary robot calibration and nonlinear compensation methodology based on GA-DNN and an extra compliance error model," Math. Probl. Eng., vol. 2020, pp. 1-15, 2020.

[23] J. Kirkpatrick, R. Pascanu, N. Rabinowitz, R. Hadsell, "Overcoming catastrophic forgetting in neural networks," Applied Mathematics, vol. 114, no. 13, pp. 3521-3526, 2017.

[24] A.A. Rusu, N.C. Rabinowitz, G. Desjardins, H. Soyer, J. Kirkpatrick, K. Kavukcuoglu, R. Pascanau, R. Hadsell, "Progressive neural networks," arXiv:1606.04671v4, pp. 1-14, 2022.

[25] S.-A. Rebuffi, A. Kolesnikov, G. Sperl, C.H. Lampert, "iCaRL: Incremental classifier and representation learning," arXiv:1611.07725v2, pp. 1-15, 2017.

[26] A. Amini, W. Schwarting, A. Soleimany, D. Rus, "Deep evidential regression," arXiv:1910.02600v2, pp. 1-20, 2020.

[27] J. Bergstra, R. Bardenet, Y. Bengio, B. Kégl, "Algorithms for hyper-parameter optimization," Proceedings of the 24th International Conference on Neural Information Processing Systems, pp. 2546-2554, 2011

[28] Hexagon AB, "Leica Absolute Tracker AT960," URL: https://hexagon.com/products/leica-absolute-tracker-at960 (Access: 2024-02-05)

[29] L. Wu, H. Ren, "Finding the kinematic base frame of a robot by hand-eye calibration using 3D position data," IEEE Transactions on Automation Science and Engineering, vol. 14, no. 1, pp. 1-11, 2016.

[30] G.A.vd. Hoorn, "ROS-Industrial support for Fanuc manipulators," URL: https://wiki.ros.org/fanuc (Access: 2023-09-05).

[31] W. Hojak, "FaRoC (Fanuc Robot Control)," URL: https://codeberg.org/hojak/FaRoC (Access: 2023-08-30).

[32] E. Uhlmann, M. Polte, J. Blumberg, "Estimation of external force-torque vector based on double encoders of industrial robots using a hybrid Gaussian process regression and joint stiffness model," Journal of Machine Engineering, vol. 23, pp. 1-13, 2023.